

AMM-161

Finite Element Simulation of Friction in Strip Ironing of High Strength Steel

Numchoak Sabangban¹, Sasawat Mahabunphachai², Sedthawatt Sucharitpwatskul², and
Numpon Mahayotsanun^{1,*}

¹ Department of Mechanical Engineering, Faculty of Engineering, Khon Kaen University, Khon Kaen 40002

² National Metal and Materials Technology Center (MTEC), Thailand Science Park, Pathum Thani 12120

*Corresponding Author: numpon@kku.ac.th, +66-87-554-2879, Fax. +66-43-202-849

Abstract

The finite element simulations of the strip ironing of high strength steel were carried out to investigate the effects of the ironing angle and the temperature to friction coefficient. Four ironing angles (5°, 10°, 15°, and 20°) were studied at three different sheet thickness (1 mm, 2 mm, and 3 mm) by keeping the reduction ratio and temperature constant at 50% and 22 °C, respectively. The range of temperature was observed by keeping the ironing angle and sheet thickness constant at 20° and 2 mm, respectively. The results showed that the friction coefficient decreased with ironing angle. At high temperature (600 °C), the friction coefficients began to decrease.

Keywords: Finite Element; Friction; High Strength Steel; Strip Ironing

1. Introduction

Advanced high strength steels (AHSS) have been growing in the automotive industry due to their effective performance in mass reduction without increased cost. In stamping of AHSS, the thickness of the sheet is normally reduced (being ironed) and the sheet-die interface is subjected to high contact pressure and increased temperature. Due to the high strength of AHSS under extreme forming condition (high contact pressure and temperature), galling on die surface usually occurs, which leads to the undesired part quality and reduced tool life. As a result, friction of the die-sheet interface in the strip ironing process of AHSS must be well understood to prevent galling.

Kawai et al. [1] developed a strip-ironing type friction testing machine to investigate the anti-

weldability of lubricants in metal forming processes and observed that this type of testing apparatus could accurately measure frictional and normal forces. The same friction testing machine was further utilized to investigate the performance of DLC-Si coating by Dohda et al. [2]. Dohda et al. [3] also developed a U-Bending-Ironing friction testing apparatus to investigate different types of coatings in ironing process. A research group at Technical University of Denmark [4-5] developed a strip reduction test based on a circular, cylindrical pin tool and obtained satisfactory results for lubricant performance screening. Delarbre and Montmitonnet [6] carried out both experimental and numerical study of the ironing of stainless steel cups and observed that the sliding velocity affected the sliding length of the drawn

AMM-161

cup on the die side to be greater than that of the punch side, causing the surface roughness on the die side to decrease much faster. Wang et al. [7] used the elasto-plastic finite element method (FEM) to investigate the surface smoothening in the ironing process and found that the plastic deformation, ironing reduction, die angle, and friction coefficient highly influenced the surface smoothening. A research group led by Altan [8-9] used the inverse Finite Element (FE) analysis by matching the punch forces obtained from the experiment to determine friction factors for different lubricants in the ironing test and this method was useful to predict the performance of each lubricant. A similar method was also utilized by Adamovic et al. [10] to determine the effects of die angle, die force, friction conditions on punch and dies, and velocity. Singh et al. [11] studied the effect of temperature in ironing process by using the FE simulation and found out that the uniform thickness distribution of the cup depended both on the temperature and deformation given to the wall thickness.

According to the aforementioned literatures, a strip ironing test was commonly used to evaluate the tribological characteristics of ironing process. In addition, many factors such as materials, sliding velocity, sliding distance, contact pressure, sheet thickness reduction ratio, ironing angle, and temperature affected the frictional behavior in ironing process. This paper aimed to establish a simple relationship between friction coefficient of the die-sheet interface and ironing angle in the strip ironing test. In addition, the temperature effect to the friction coefficient was also investigated. The understanding of friction

behaviors in strip ironing from this study will be beneficial to the automotive industry in order to optimize the materials, processes, and costs in stamping of high strength steel.

2. Finite Element Simulation

A schematic of the one-sided strip ironing test used in this study is displayed in Fig. 1(a) and the geometry of the test is shown in Fig. 1(b). The friction coefficient of the die-sheet interface can be established as shown in Eq. (1).

$$\mu = (F_p \cos\alpha - 2F_d \sin\alpha) / (F_p \sin\alpha + 2F_d \cos\alpha) \quad (1)$$

Where μ is the friction coefficient of the die-sheet interface, F_p is the punch force, F_d is the die force, α is the ironing angle. The reduction ratio (R_e) can be calculated from Eq. (2).

$$R_e = (t_1 - t_2) * 100\% / t_1 \quad (2)$$

Where t_1 is the original sheet thickness and t_2 is the final sheet thickness. Note that R_e is kept constant at 50% throughout this study.

A finite element (FE) model was established as shown in Fig. 2(a) by using MSC.Marc. The 2D non-linear plane strain thermal/structural approach was selected. The punch and die were modelled as rigid bodies. The sheet was modelled as a deformable body. The selected die and sheet material properties were based on [12] and the property values used in the FE simulation are presented in Table 1. Note that E is the Young's Modulus, Y is the yield strength, K is the material constant, and n is the strain hardening exponent.

AMM-161

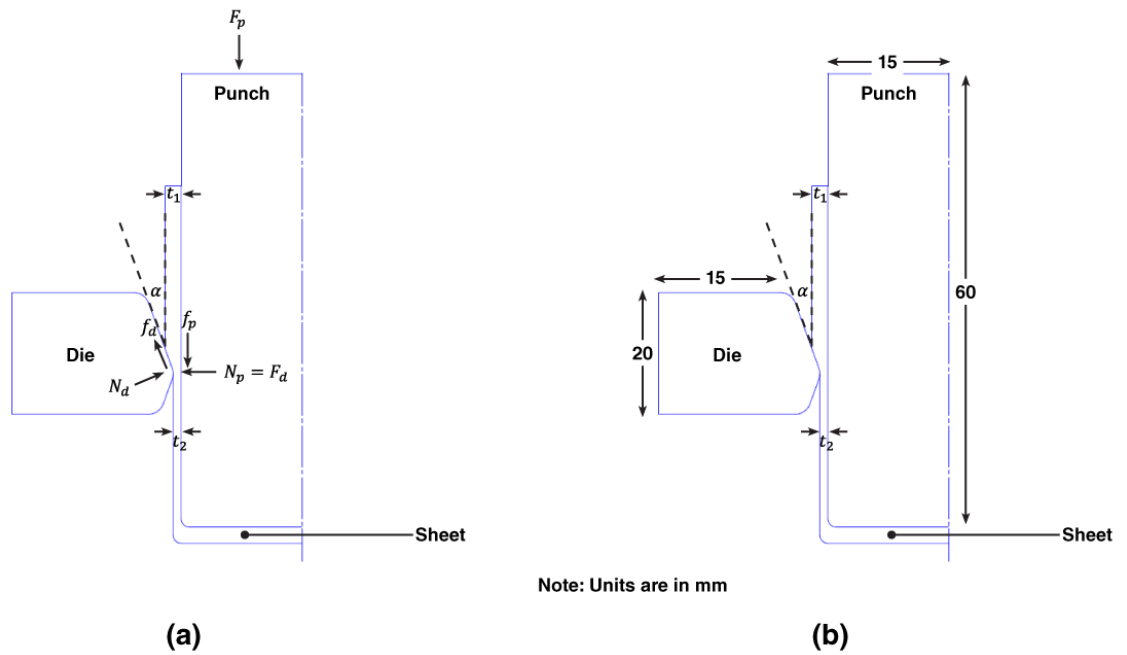


Fig. 1 (a) Schematic of the strip ironing test; and (b) geometry of the strip ironing test

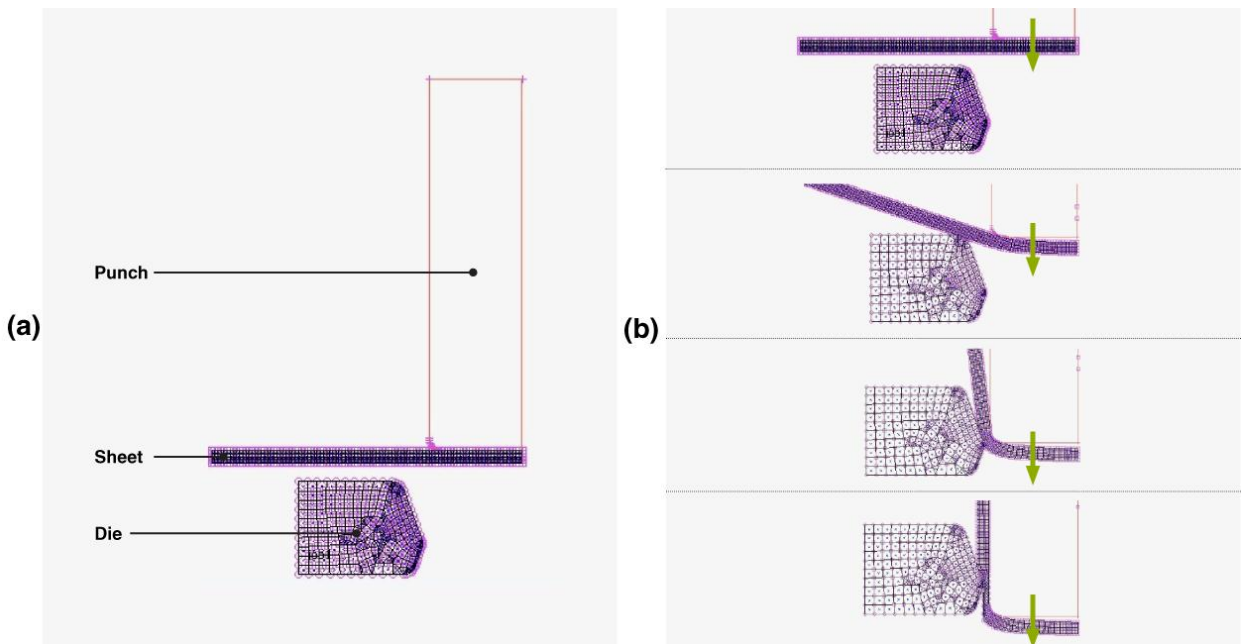


Fig. 2 (a) FE model of the strip ironing test; (b) various steps in the FE simulation

The thermal properties of the sheet material used to investigate the thermal effects (22 °C to 940 °C) are presented in Table 2. The overall heat transfer coefficient, conductivity, specific

heat capacity, and emissivity coefficient of the sheet were set to be $25 \text{ W(m}^2\text{K)}^{-1}$, $43 \text{ W(m}^2\text{K)}^{-1}$, $0.49 \text{ kJ(kgK)}^{-1}$, and 0.79, respectively. Note that the die temperature was set to be constant at

AMM-161

200 °C for all sheet temperatures except for the 22 °C case.

The arctangent friction model was selected for the die-sheet interface and the chosen friction coefficient was 0.3, representing commonly used value for dry condition between die and sheet in strip ironing [10]. During the FE simulation, the punch was moved vertically downward at 5 mm/s to form the sheet into the ironing die and the total travel punch displacement was 70 mm as shown

in different steps in Fig. 2(b). The obtained punch and die forces were calculated to determine the friction coefficient between the die-sheet interface during the punch travel. Two main factors were considered here: (1) ironing angle (α) and (2) temperature and the simulation conditions investigating these factors are presented in Tables 2 and 3.

Table. 1 Material properties of die and sheet used in the FE simulation

Temperature (°C)	Sheet				Die	
	E (N/mm ²)	Y (N/mm ²)	K (N/mm ²)	n	E (N/mm ²)	Y (N/mm ²)
22	223000	777	900	0.0213	2×10^{14}	1×10^{14}
60	231900	776	900	0.0237		
120	225230	750	900	0.0294		
150	232000	731	900	0.0334		
180	227000	678	900	0.0455		
240	218000	702	1000	0.0641		
300	223000	648	1000	0.0698		
410	205000	693	1000	0.0579		
460	209000	801	900	0.0187		
540	194000	627	700	0.0175		
600	162790	469	500	0.0103		
660	162800	378	400	0.0090		
720	114000	153	200	0.0423		
770	109000	81	100	0.0332		
830	73500	61	90	0.0536		
940	26700	36	40	0.0187		

Table. 2 Simulation conditions investigating the ironing angle factor

AMM-161

Parameter	Value
Sheet thickness (mm)	1.0, 1.5, 2.0
Temperature (°C)	22
Ironing angle (°)	5, 10, 15, 20

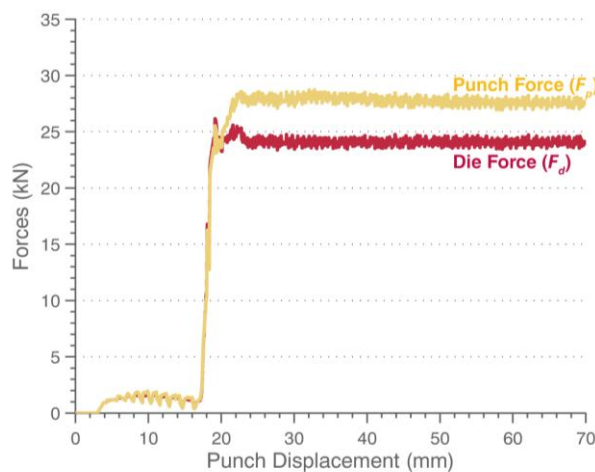
Table. 3 Simulation conditions investigating the temperature factor

Parameter	Value
Sheet thickness (mm)	2.0
Ironing angle (°)	20
Temperature (°C)	22, 60, 120, 150, 180, 240, 300, 410, 460, 540, 600, 720, 770, 830, 940

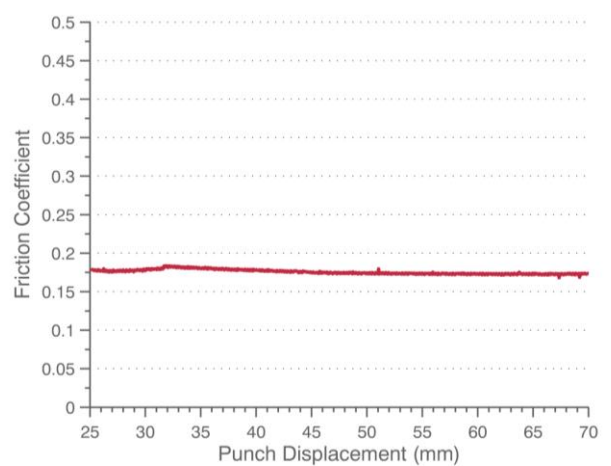
3. Results and Discussions

An example of the obtained punch and die forces from a simulation is shown in Fig. 3(a). Initially, the forces required to move the sheet downward were very small until the sheet made contact to the die (18 mm) when the forces increased. Then, the constant forces were obtained after the sheet was being ironed (22

mm). The forces during the ironing stage were considered (25 to 70 mm) and the friction coefficients (calculated by Eq. (1)) could be obtained as shown in Fig. 3(b). Note that only the friction coefficients in the ironing stage (25 to 70 mm) were used for comparison throughout this study.



(a)



(b)

Fig. 3 The FE results of the strip ironing test of 2 mm sheet thickness at 22 °C and 20° ironing angle: (a) punch and die forces vs. punch displacement; and (b) friction coefficient vs. punch displacement

AMM-161

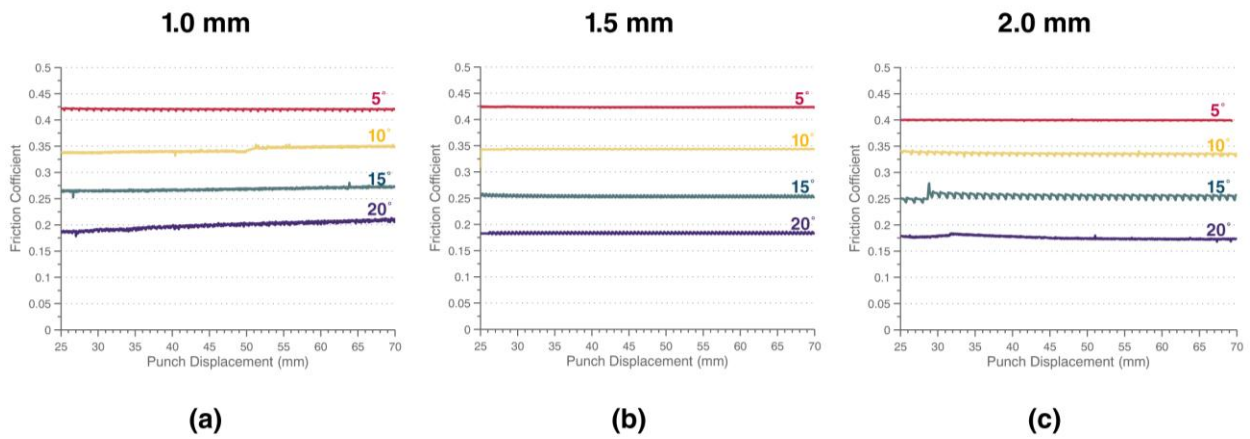


Fig. 4 Friction coefficient vs. punch displacement of the strip ironing test of at 22 °C at different ironing angles: (a) 1.0 mm sheet thickness; (b) 1.5 mm sheet thickness; (c) 2.0 mm sheet thickness

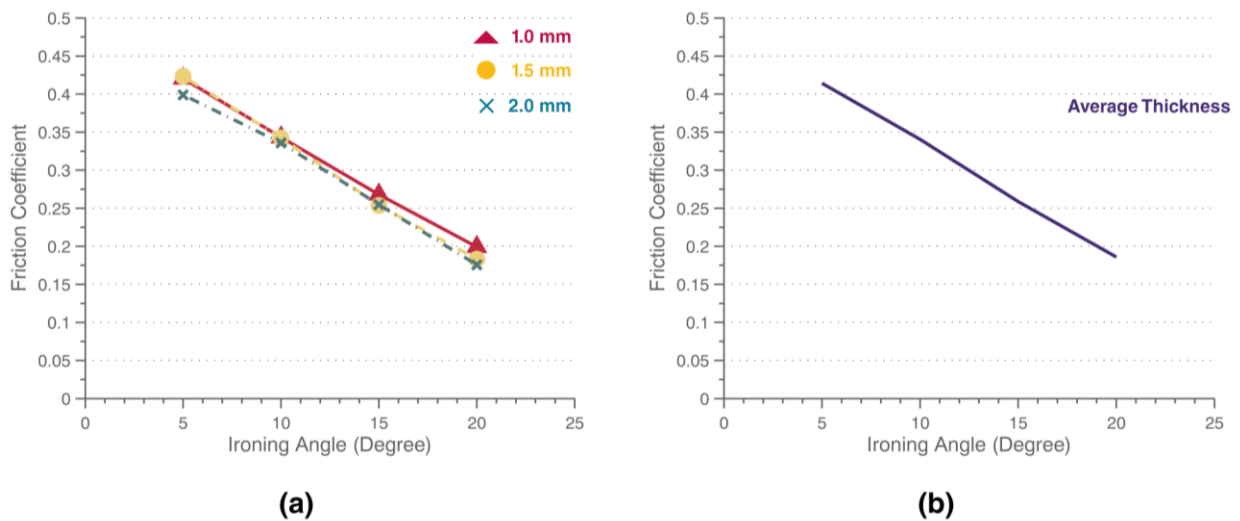


Fig. 5 Relationship between the friction coefficient and ironing angle: (a) three sheet thickness; and (b) average thickness

3.1 Effect of Ironing Angle

The effect of the ironing angle could be observed in Figs. 4 and 5. The friction coefficient decreased with increasing ironing angle for all three sheet thickness. It could also be observed that varying the sheet thickness did not significantly affect the friction coefficients because the reduction ratio was kept constant for all cases.

The friction coefficients of the three sheet thickness were averaged at each ironing angle and plotted as shown in Fig. 5(b). According to Eq. (1), the friction coefficient is dependent on the ironing angle, punch force, and die force. In order to verify the simulation results, the friction coefficients at different ironing angles must be compared with those of the analytical calculation

AMM-161

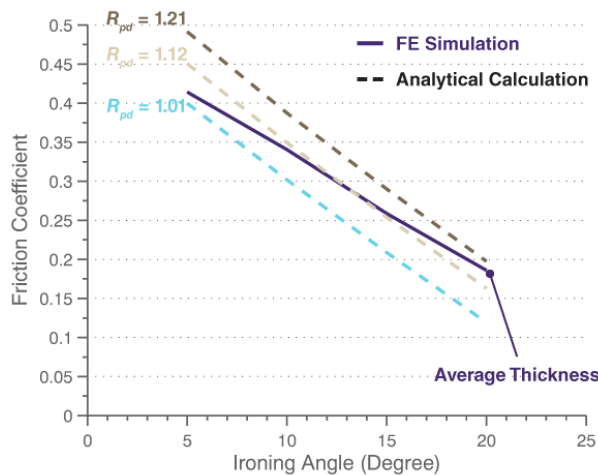
obtained from Eq. (1). If the ratio of the punch force over die force ($R_{pd} = F_p/F_d$) is established, Eq. (1) can be rewritten as:

$$\mu = (R_{pd}\cos\alpha - 2\sin\alpha)/(R_{pd}\sin\alpha + 2\cos\alpha) \quad (3)$$

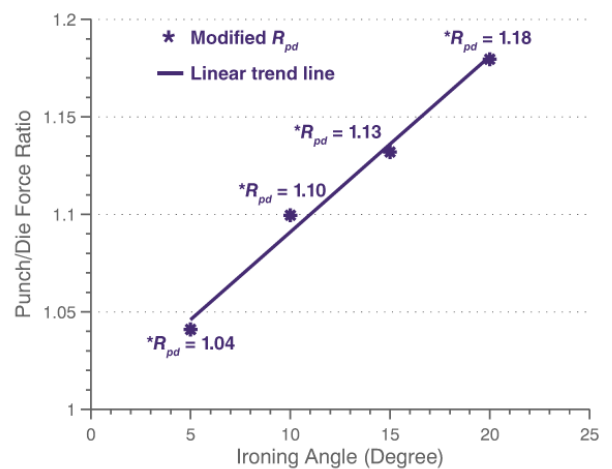
Based on the simulation results, the values of R_{pd} ranged from 1.01 to 1.21, which were also selected to determine the values of the analytical friction coefficients. The comparison between the simulation and the analytical results of the friction coefficients at the selected values of R_{pd} is illustrated in Fig. 6 (a). It could be observed that the simulation results provided the same trend as that of the analytical calculation and fell into the

selected range of R_{pd} . It should also be noted that R_{pd} is not always constant at all ironing angles and the values of the punch and die forces must be obtained from and validated with the actual strip ironing experiment. However, if the friction behavior of the experimental results is similar to that of the simulation shown in Fig. 6(a), it is interesting to note that R_{pd} changes with ironing angle. As a result, the values of R_{pd} can be modified to match the correct value of the simulation by the following equation, which is also shown in Fig. 6(b).

$$*R_{pd} = 0.009\alpha + 1.001 \quad (4)$$



(a)



(b)

Fig. 6 (a) Friction coefficient vs. ironing angle of different values of R_{pd} ; and (b) Modified R_{pd} vs. ironing angle

3.2 Effect of Temperature

The effect of temperature can be seen in Fig. 7. Based on the simulation results, it could be noticed that friction coefficient began to drop around 600 °C. Note that the obtained friction

coefficients in this study were mainly dependent on the punch force, die force, and ironing angle. This also implied that the R_{pd} values decreased at high temperature. Previous works demonstrated that the friction coefficient could increase or

AMM-161

decrease with temperature depending on the operating conditions, coatings, and lubrication [13-16]. Since the simulation in this study only considered the influence of temperature to the die and sheet materials, the results simply indicated that temperature slightly affected the overall friction coefficients. In order to better observe the temperature effect, wear and friction phenomena including the oxide layers at elevated temperatures must be included in the simulation, which is the future work of this study.

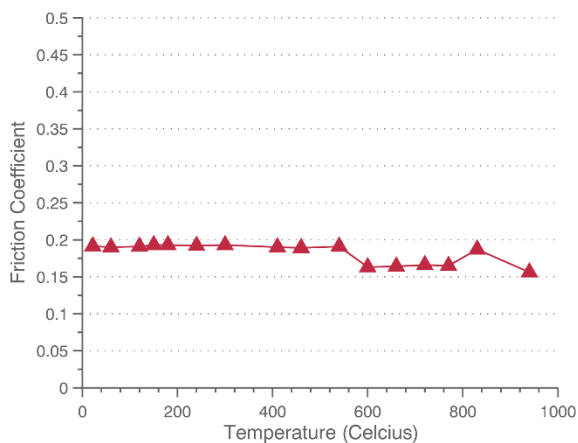


Fig. 7 Friction coefficient vs. temperature of the strip ironing test of 2 mm sheet thickness at 20° ironing angle

6. Conclusions

The FE simulations of the strip ironing were carried out to investigate the effects of ironing angle and temperature. The results showed that the friction coefficient decreased with ironing angle. In addition, the ratio of the punch force and die force, which affected the friction behavior, also increased with ironing angle. At high temperature (600 °C), the friction coefficient started to drop.

6. Acknowledgement

The authors would like to acknowledge the supports from Department of Mechanical Engineering, Faculty of Engineering, Khon Kaen University (KKU) and National Metal and Materials Technology Center (MTEC). In addition, the authors would like to sincerely thank Prof. Kuniaki Dohda (Northwestern University, USA) and Mr. Sukunthakan Ngernbamrung (MTEC) for their suggestions and advice.

7. References

- [1] Kawai, N., Nakamura, T., and Dohda, K. (1982). Development of anti-weldability test in metal forming by means of strip-ironing type friction testing machine. *Journal of Engineering for Industry*, vol.104(4), November 1982, pp. 375-382.
- [2] Dohda, K., Kubota, H., and Tsuchiya, Y. (2005). Application of DLC coating to ironing die. *JSME International Journal*, vol.48(4), pp. 286-291.
- [3] Dohda, K., Makino, T., and Katoh, H. (2009). Tribo-Characteristic of coated die against magnesium in ironing process. *ESAFORM 2009*, vol.2, pp. 243-246.
- [4] Andreasen, J. L., Bay, N., Andersen, M., Christensen, E., and Bjerrum, N. (1997). Screening the performance of lubricants for the ironing of stainless steel with a strip reduction test. *Wear*, vol.207(1-2), pp. 1-5.
- [5] Petrushina, I. M., Christensen, E., Bergqvist, R. S., Møller, P. B., Bjerrum, N. J., Høj, J., Kann, G., and Chorkendorff, I. (2000). On the chemical nature of boundary lubrication of stainless steel by chlorine- and sulfur-containing EP-additives. *Wear*, vol.246(1-2), pp. 98-105.

AMM-161

- [6] Delarbre, D. and Montmitonnet, P. (1999). Experimental and numerical study of the ironing of stainless steel cups. *Journal of Materials Processing Technology*, vol.91(1-3), pp. 95-104.
- [7] Wang, Z., Dohda, K., and Jeong, Y. (2001). FEM simulation of surface smoothing in the ironing process. *Journal of Materials Processing Technology*, vol.113(1-3), pp. 705-709.
- [8] Chandrasekharan, S., Palaniswamy, H., Jain, N., Ngaile, G., and Altan, T. (2005). Evaluation of stamping lubricants at various temperature levels using the ironing test. *International Journal of Machine Tools and Manufacture*, vol.45(4-5), pp.379-388.
- [9] Kim, H., Altan, T., and Yan, Q. (2009). Evaluation of stamping lubricants in forming advanced high strength steels (AHSS) using deep drawing and ironing tests. *Journal of Materials Processing Technology*, vol.209(8), pp. 4122-4133.
- [10] Adamovic, D., Mandic, V., Jurkovic, Z., Grizel, B., Stefanovic, M., Marinkovic, T., and Aleksandrovic, S. (2010). An experimental modelling and numerical fe analysis of steel-strip ironing process. *Technical Gazette*, vol.17(4), pp. 435-444.
- [11] Singh, S. K., Kumar, V., Prudvi Reddy, P., and Gupta, A. K. (2014). Finite element simulation of ironing process under warm conditions. *Journal of Materials Research and Technology*, vol.3(1), pp. 71-78.
- [12] Chen, J., Young, B., and Uy, B. (2006). Behavior of high strength structural steel at elevated temperatures. *Journal of Structural Engineering*, vol.132(12), pp. 1948-1954.
- [13] Hardell, J., Kassfeldt, E., and Prakash, B. (2008). Friction and wear behaviour of high strength boron steel at elevated temperatures of up to 800°C. *Wear*, vol. 264(9-10), pp. 788-799.
- [14] Ghiotti, A., Bruschi, S., and Borsetto, F. (2011). Tribological characteristics of high strength steel sheets under hot stamping conditions. *Journal of Materials Processing Technology*, vol. 211(11), pp. 1694-1700.
- [15] Yanagida, A., Kurihara, T., and Azushima, A. (2010). Development of tribo-simulator for hot stamping. *Journal of Materials Processing Technology*, vol. 210(3), pp. 456-460.
- [16] Geiger, M., Merklein, M., and Lechler, J. (2008). Determination of tribological conditions within hot stamping. *Production Engineering. Research and Development*, vol. 2(3): pp. 269-276.